Preparation and Properties of Poly(methyltrifluoropropylsiloxane-*b*-imide) Copolymer. I

DOO WHAN KANG,[1] YOUNG MIN KIM[2]

[1] Hyperstructured Organic Materials Research Center, Department of Polymer Science & Engineering, Dankook University, Hanmandong San 8, Yongsangu Seoul 140-714, Korea

[2] Department of Chemical Engineering, Dankook University, Hanmandong San 8, Yongsangu Seoul 140-714, Korea

Received 30 May 2001; accepted 28 August 2001

ABSTRACT: Poly(methyltrifluoropropylsiloxane-*block*-imide) copolymers (PSBPI), containing various contents of fluorosiloxane, were prepared by the thermal imidization of 3,3′,4,4′-benzophenonetetracarboxylic dianhydride (BTDA), 4,4′-oxydianiline (ODA), and α,ω-aminopropyl-terminated poly(methyltrifluoropropylsiloxane) prepolymer (APMFS). APMFS was prepared from an equilibrium polymerization of (3,3,3-trifluoropropyl)methylcyclotrisiloxane ($D_3^{Me,CH2,CH2,CF3}$) with 1,3-bis(3-aminopropyl)-1,1,3,3-tetramethyldisiloxane in the presence of the tetramethylammoniumhydroxide (TMAH) catalyst. The content of APMFS, in the reaction mixture, was varied from 0 to 30 wt % of diamine. The structure of copolymer was confirmed by FTIR spectroscopy. The thermal stability, linear coefficient of thermal expansion, modulus, X-ray pattern, and other properties, such as surface enrichment behavior and solubility, were investigated. PSBPI exhibited relatively low crystallinity regardless of the APMFS content in the copolymer. On the other hand, thermogravimetric, thermomechanical, dynamic mechanical, and surface properties were affected by the content of APMFS segment in the copolymer backbone. © 2002 Wiley Periodicals, Inc. J Appl Polym Sci 85: 2867–2874, 2002

Key words: polyimide; block copolymers; FTIR

INTRODUCTION

Polyimides are some of the most widely used polymers, particularly in aerospace, microelectronics, printed circuit, and high-performance adhesive industries. This is due to their excellent thermal stability and mechanical strength. After imidization, however, they have properties that inhibit processability, insolubility, intractability, and high glass transition temperature.[1–4] In the last decade, several copolyimides containing polyorganosiloxane in their copolymer backbone, as block units, have been prepared to improve processing, and they have been applied in high-performance adhesives and special coatings.[5–8] Recently, some copolyimides containing polyorganofluorosiloxane have been reported that exhibit low dielectric constants. In this study, polyorganosiloxane-b-polyimide copolymer containing α,ω-aminopropyl terminated poly(methyltrifluoropropylsiloxane) prepolymer (APMFS) was prepared from the thermal imidization of APMFS with 3,3′,4,4′-benzophenonetetracarboxylic dianhydride (BTDA) and 4,4′-oxydianiline (ODA). The structures of APMFS and copolyimide were confirmed by Fourier transform infrared spectroscopy (FTIR) and nuclear magnetic resonance spectroscopy (NMR), and the

Correspondence to: Y. M. Kim (kdoowh@dankook. ac.kr).
Contract grant sponsor: Hyperstructured Organic Materials Research Center.

Journal of Applied Polymer Science, Vol. 85, 2867–2874 (2002)

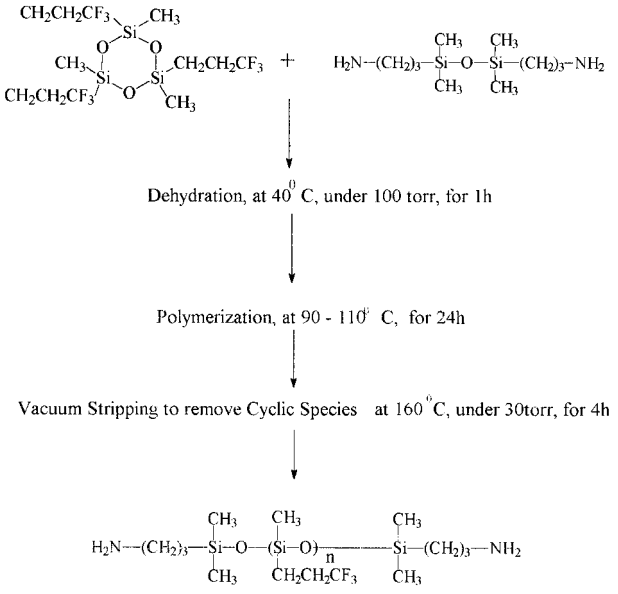

Scheme 1 Preparation of APMFS.

thermal and mechanical properties were measured by differential scanning calorimeter (DSC), dynamic mechanical analysis (DMA), thermomechanical analysis (TMA), and a mechanical tester. The surface topography of the copolyimide film, according to the content of APMFS, was measured by atomic force microanalysis (AFM) and scanning electron microscopy (SEM).

EXPERIMENTAL

Materials and Reagents

3,3,3-Trifluoropropyl)methylcyclotrisiloxane was purchased from Gelest Co. 1,3-Bis(3-aminopropyl)-1,1,3,3-tetramethyldisiloxane was supplied from United Chemical Technology. They were used without further purification, and stored under pressurized nitrogen. Tetramethylammoniumhydroxide (TMAH), from Fluka Co., was used as received. 3,3′,4,4′-Benzophenonetetracarboxylic dianhydride (BTDA) was supplied from Al-

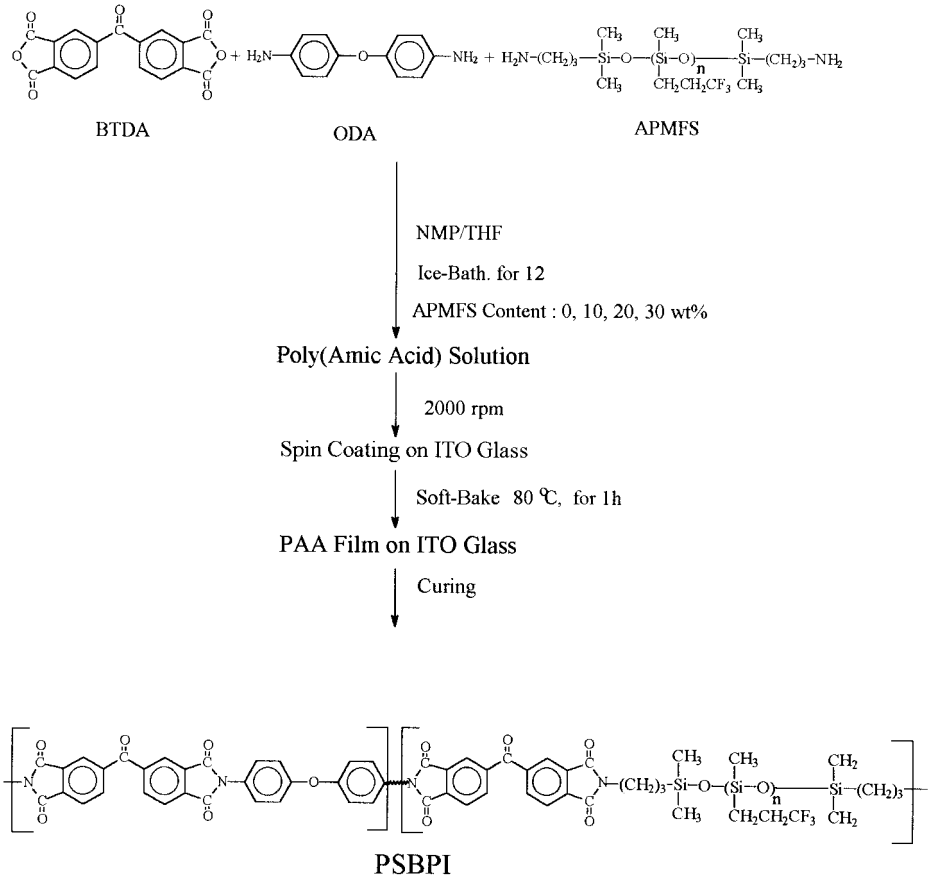

Scheme 2 Preparation of PSBPI by thermal imidization.

Table I Curing Conditions for PSBPI

		Film Formation			
	Solvent	Soft-Bake (80°C, 30 min)	Soft-Bake (80°C, 60 min)	Curing Rate (2°C/min)	Coring Rate (2°C/min)
Pure PI	NMP	Yes	Yes	Yes	Yes
PSBPI (APMFS, 10 wt %)	NMP/THF	Crack	Yes	Yes	Crack
PSBPI (APMFS 20 wt %)	NMP/THF	Crack	Yes	Yes	Crack
PSBPI (APMFS, 30 wt %)	NMP/THF	Crack	Yes	Yes	Crack

drich Co., and it was further purified by recrystallization using acetic anhydride. 4,4′-Oxydianiline (ODA), from Tokyo Kasei Co., was recrystallized from ethyl alcohol prior to use, and was dried in a vacuum oven at 90°C for 24 h. *N*-Methyl-2-pyrrolidinone (NMP), obtained from Fisher Co., was purified from vacuum distillation after drying over P_2O_5 and stored over molecular sieves (4 Å) under nitrogen atmosphere.

Preparation of APMFS

APMFS was prepared from an equilibrium polymerization reaction of $D_3^{Me,CH2,CH2,CF3}$ and 1,3-bis(3-aminopropyl)-1,1,3,3-tetramethyldisiloxane with a 6 to 1 mol ratio, respectively, in the presence of 0.02 wt % of TMAH at 90°C for 24 h. After completing the reaction, the reaction mixture was heated to 160°C to decompose TMAH, and then it was vacuum stripped to remove any cyclic species and TMAH at 30 Torr for 4 h (yield: 67%).

Preparation of PSBPI

APMFS was added to a four-necked flask equipped with a mechanical agitator, thermometer, condenser, and a nitrogen inlet tube containing a solution of ODA in NMP/THF (80 : 20 volume ratio) mixed solvent. The reaction was carried out for 12 h in ice-water bath after adding BTDA slowly for 30 min. APMFS was incorporated into the BTDA–ODA backbone at a concentration from 0 to 30 wt % of diamine. The solid contents of resulting solutions were approximately 15 wt %. Each of the produced poly(amic acid) solutions was filtered using a 0.2-μm syringe filter, deposited on rinsed ITO glass, and spin-coated at a speed of 2000 rpm for 10 s. The

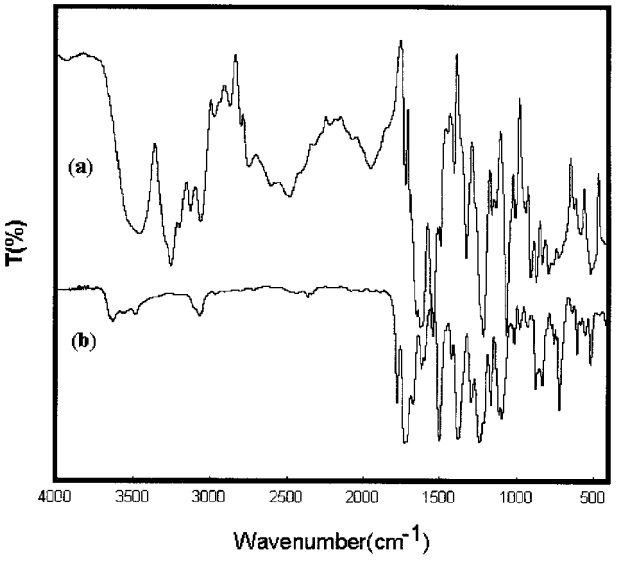

Figure 1 FTIR spectra of poly(amic acid) (a) and PSBPI (b).

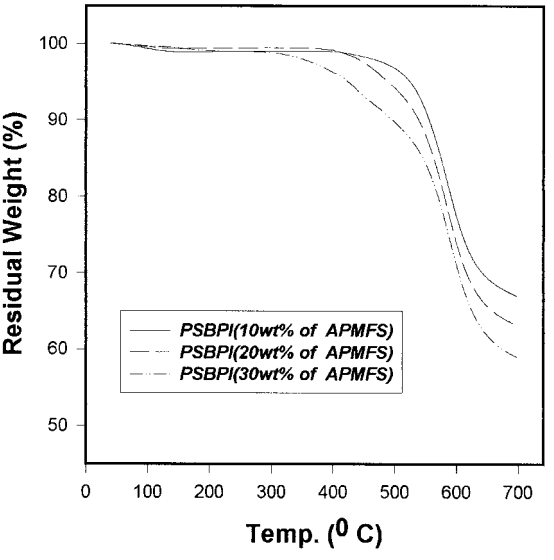

Figure 2 TGA spectra of PSBPI according to the content of APMFS.

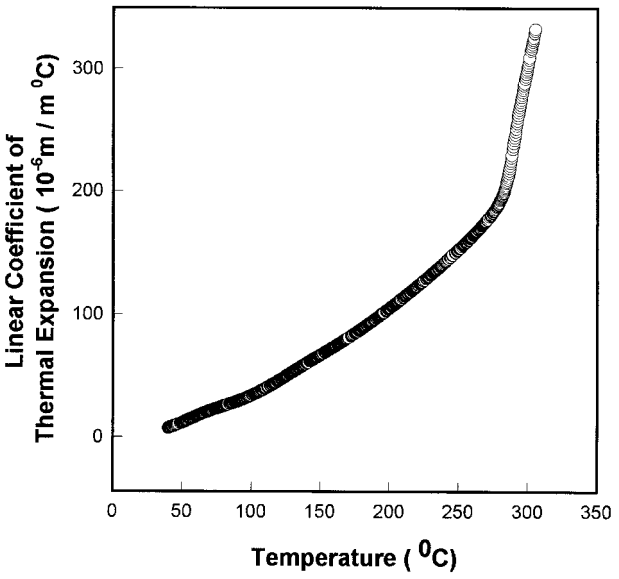

Figure 3 TMA result of PSBPI according to the content of APMFS.

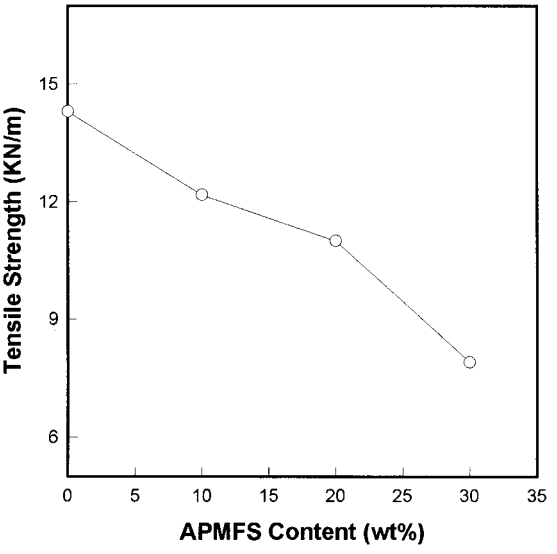

Figure 4 Tensile strength of PSBPI according to the content of APMFS.

coated poly(amic acid) solutions were soft baked at 80°C for 1 h. The half dried films were cured from 80 to 350°C at a heating rate of 2°C/min, and then held at 350°C for 1 h. The thicknesses of the imidized films were adjusted to the level of 4–5 μm. The films were then finally peeled off from ITO glass substrate by immersing in boiling water.

Characterization

The FTIR spectra were obtained from KBr pellets of the samples using an FTIR spectrometer (Perkin-Elmer Spectra GX). The ^{1}H-NMR spectrum was obtained from the sample containing tetramethylsilane (TMS) 0.01% in $CDCl_3$ solution using a NMR spectrometer (Varian EM-360A). TMA was performed using a TA Instrument 2100 TMA at a scan rate of 20°C/min, and a quartz probe weighted with 0.2 *N*. TGA experiments were conducted using a TA Instrument 2100 TGA with automated sample changer, scan rate of 10°C/min, in a nitrogen purge. The lower and upper glass transition temperatures (T_g) due to APMFS and BTDA–ODA segments were determined by the DMA using a Perkin-Elmer 7. They were analyzed from −150 to 400°C at a heating rate of 5°C/min and at a frequency of 1 Hz. The surface morphology of the PSBPI films was studied by using an SEM (Hitachi Co.). The samples were coated with gold to enhance their conductivity, which gave good resolution of the images. AFM, using a microscope of Digital Instrument Co., Japan, was measured with a contact angle mode.

Table II. Linear Coefficient of Thermal Expansion and T_g for PSBPI

	PSBPI (APMFS 10 wt %)	PSBPI (APMFS 20 wt %)	PSBPI (APMFS 30 wt %)
CTE (μm/m°C)	161	102	59
T_g	271	254	184

Surface treatment of ITO Glass

ITO glass was soaked in HCl/H_2NO_3 (9 : 1 volume ratio) solution for 4 h, rinsed with deionized water and tetrachloroethane. Then, it was rinsed again with acetone, methyl alcohol, and vacuum dried at 50°C for 1 h.

RESULTS AND DISCUSSION

Preparation of APMFS

APMFS was prepared from an equilibrium polymerization of $D_3^{Me,CH2,CH2,CF3}$ and 1,3-bis(3-aminopropyl)-1,1,3,3-tetramethyldisiloxane in the presence of the TMAH catalyst as previously reported.[9] The reaction mechanism of APMFS is shown in Scheme 1. With increased reaction time, the re-

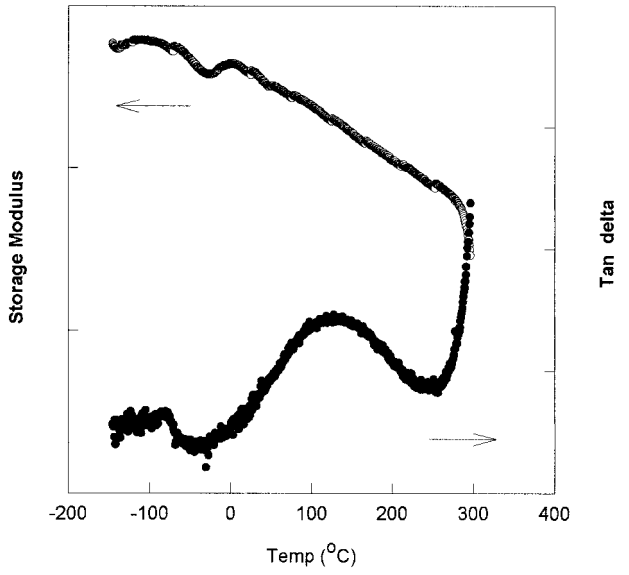

Figure 5 Dynamic mechanical spectrum of PSBPI containing APMFS (20 wt %).

action mixture was transformed into a viscous and transparent solution. It was found that reaction mixture polymerized gradually and became more miscible with sufficient reaction time. The structure was confirmed by FTIR and a ^{1}H-NMR spectrometer.

Preparation of PSBPI

PSBPI, containing various contents of fluorosiloxane segment in PI backbone, was prepared by the thermal imidization of BTDA, ODA, and APMFS. The reaction mechanism for dianhydride, diamine, and amine-terminated polyorganofluorosiloxane prepolymer is shown in Scheme 2. When BTDA was added to ODA/APMFS solution, the reaction was exothermic due to the reaction of BTDA. Thus, it was necessary to decrease the reaction temperature, near to 0°C produce high viscous poly(amic acid) solution. NMP/THF mixed solvent was used in the preparation of the poly(amic acid) solution containing APMFS in BTDA–ODA backbone. Mixed solvent played an important role in enhancing the solubility and maintaining the homogeneous phase of reactants. Transparent PSBPI films were prepared by varying the curing conditions, as shown in Table I. In Table I, the optimum soft baking condition was heating poly(amic acid) solutions, containing APMFS in the backbone, at 80°C for 60 min, and then curing them to 350°C at a rate of 2°C/min. Films were then held at 350°C for 1 h. From these results, it was shown that insufficient soft baking time and a rapid curing rate can affect the complete removal of water and residual solvent from coating, leading to cracking or shrinkage. The FTIR spectrum of PSBPI is illustrated in Figure 1. Figure 1 shows that the absorption peaks due to the symmetric and unsymmetric stretching vibration of C═O appeared at 1778 and 1728 cm^{-1}. The absorption peak due to the stretching vibration of C—N appeared at 1370 cm^{-1}, and the absorption peak due to the bending vibration of C═O appeared at 728 cm^{-1}. Noticeably, the new absorption peak due to Si—OH appeared at 3350–3600 cm^{-1}. On the other hand, the peak intensities due to symmetric and unsymmetric stretching vibrations of —CH_3 in Si—CH_3 decreased at 2910 and 2970 cm^{-1}. From these re-

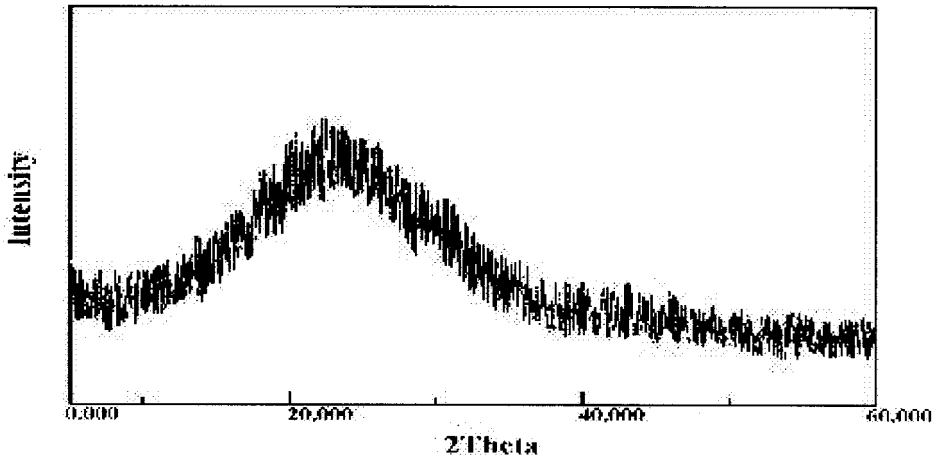

Figure 6 Wide-angle X-ray scattering curve of PSBPI.

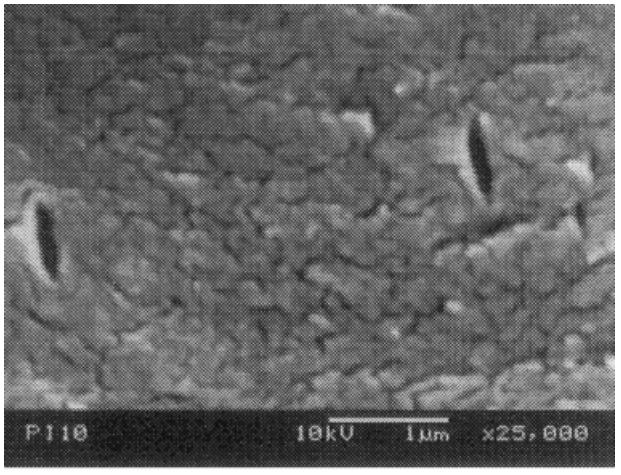

(a)

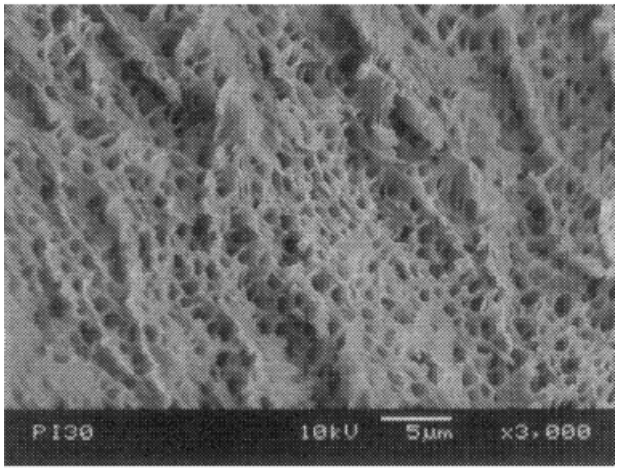

(b)

Figure 7 SEM images of PSBPI containing 10 wt % (a) and 30 wt % (b).

sults, it was concluded that the APMFS segment migrated out of the surface of the coating, because it had a lower surface energy than that of the BTDA–ODA segment. It was interesting to note that the Si—CH_3 group, in the APMFS segment, was converted to Si—OH at 180°C.[10]

Thermogravimetric Properties

The thermal stabilities of the PSBPI were measured by TGA under nitrogen atmosphere. TGA curves of PSBPI are shown in Figure 2. TGA analysis for various PSBPI shows that residual weight (Wtr) of PSBPI with a higher composition of APMFS in the BTDA–ODA backbone decreased from 67% (APMFS content: 10 wt %) to 59% (APMFS content: 30 wt %) at 700°C, and the initial thermal degradation temperature (T_d) was observed at a lower temperature as the APMFS content increased. From these results, it was interesting to note that thermal stabilities of PSBPI were a function of content of the incorporated APMFS segment. Additionally, it was concluded that T_d was caused by the propyl group and also shifted to a lower temperature with increasing APMFS content, because the propyl group in the APMFS segment was thermally unstable.

Thermomechanical Properties

The linear coefficient of thermal expansion (CTE, α) and glass transition temperature (T_g) were measured by TMA under nitrogen atmosphere, where α is the slope of the relative dimension change to temperature curve, and T_g is the inflection point between two lines. TMA results are illustrated in Figure 3 and Table II, respectively: α decreased from 161 to 59 μm/m°C. T_g decreased from 271 to 184°C. These results are due to Si—OH groups generated from the Si—CH_3 groups undergoing considerable intercrosslinking reaction as the content of APMFS increased. From these results, one can see that PSBPI with a high content of APMFS segment behaved as a thermoplastic elastomer, and thermo-mechanical properties of PSBPI were dependent on the weight contents of APMFS and BTDA–ODA segments. Figure 4 shows the results of tensile strength for PSBPI: as shown in Figure 4, the tensile strength of PSBPI decreased with increasing flexible APMFS segment content.

Dynamic Mechanical Properties

The lower and upper thermal transition phenomena were confirmed by DMA. A representative DMA spectrum is depicted in Figure 5. In Figure 5, microphase separation phenomenon between APMFS and the BTDA–ODA segment is shown: PSBPI has two dropping inflection points of storage modulus (E') corresponding to two peaks of tan δ. The peak in the tan δ curve at around -80°C, was due to the lower T_g from the soft segment of APMFS, and was accompanied by a decrease in modulus. The lower T_g, due to the APMFS segment, did not change as a function of content, except for changes of modulus. On the other hand, the upper T_g, due to the hard segment of BTDA–ODA, depended on the APMFS content,

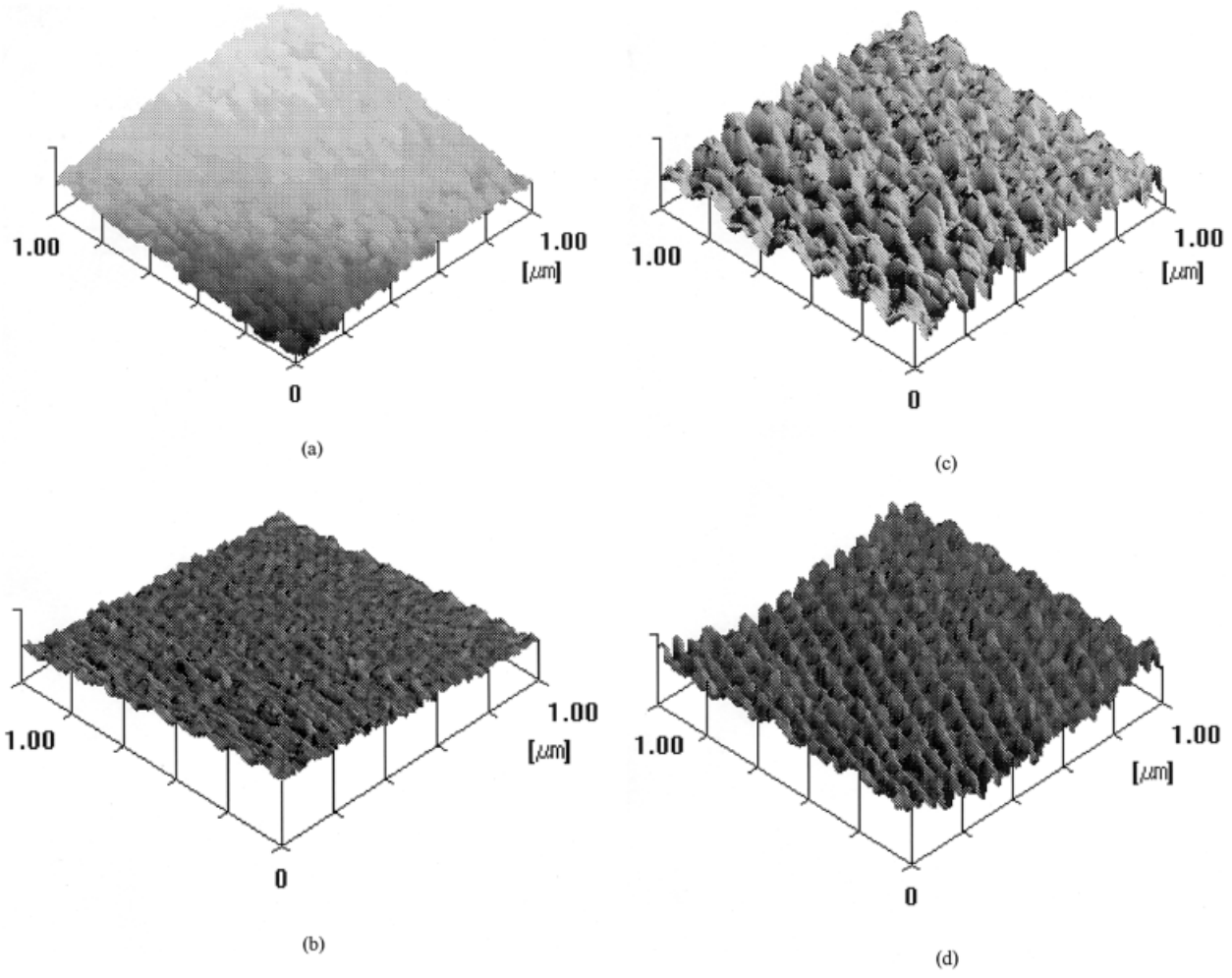

Figure 8 Surface topography of PSBPI containing APMFS content of 0 wt % (a), 10 wt % (b), 20 wt % (c), and 30 wt % (d).

and it was fully consistent with the TMA result and was attributed to the relaxations between the soft APMFS segment and the hard BTDA–ODA segment.

Wide-Angle X-ray Diffraction Pattern

All the optically transparent PSBPI films were structurally characterized by the wide-angle X-ray diffraction method. This result is presented in Figure 6. As Figure 6 indicates, all the PSBPI films had similar diffraction patterns and exhibited diffraction peaks with a big amorphous halo at around 3–40° (2θ). The diffraction peak was weak, and showed that PSBPI films had relatively low crystallinity.

Surface Properties

The morphology of the cross-section for PSBPI was examined by SEM, as shown in Figure 7. In Figure 7, images (a) and (b) are the morphology of PSBPI containing 10 and 30 wt % of APMFS into the BTDA–ODA backbone, and also show different morphology patterns: microphase separation phenomenon between the APMFS segment and BTDA–ODA segment occurred to form a rough surface at the content of 10 wt % of APMFS. On the other hand, when the content of APMFS increased up to 30 wt %, quite well-distributed APMFS domains, attributed to the formation of a smooth surface, were observed on the surface of PSBPI. These results were consistent with the surface topography and the surface roughness obtained from AFM. The surface topography and the surface roughness factor (Ra) of PSBPI are depicted in Figures 8 and 9, respectively. Shown in Figure 8(a) is the surface of homo PI containing only the BTDA–ODA segment: it is very even and smooth (Ra: 0.22 μm). All the surfaces of PSBPI,

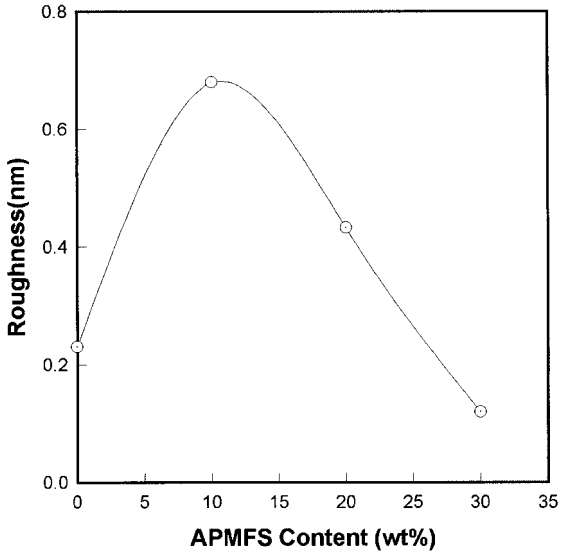

Figure 9 Ra for the PSBPI according to APMFS content.

except for (a), were enriched in APMFS domains called "islands" in the sea, and exhibited different roughnesses. Roughness decreased as the content of APMFS increased from 10 to 30 wt %. Especially, in the case of PSBPI (b) containing 10 wt % of APMFS, APMFS domains were not well distributed on the surface of PSBPI, and Ra reached a plateau (Ra: 0.68 μm). On the other hand, as shown in Figure 8(d), the surface of PSBPI containing 30 wt % of APMFS exhibited smooth topography to form a continuous phase in the surface. Therefore, its Ra gradually decreased with increasing content of APMFS, 10–30 wt % in PSBPI, and was analogous to that of homo PI containing only the BTDA–ODA segment. This was due to APMFS domains being continuously distributed. From these results it is concluded that the microphase separation phenomenon occurred between the soft APMFS and the hard BTDA–ODA segment due to the difference of the solubility parameter, the surface energy, and the content of incorporated APMFS content in the PI backbone.

Solubility Properties

The solubility of various PSBPIs containing APMFS in the PI backbone in many kinds of organic solvents were determined for a 0.1% (wt/vol) concentration. All of the prepared PSBPI were insoluble in organic solvents, except for the aprotic polar solvents, such as dimethylformamide (DMF), dimethylsulfoxide (DMSO), dimethylacetamide (DMAc), and *N*-methyl-2-pyrrolidone (NMP).

CONCLUSIONS

PSBPI containing various contents of APMFS were prepared by the thermal imidization of BTDA, ODA, and APMFS. APMFS was prepared from an equilibrium polymerization reaction of $D_3^{Me,CH2,CH2,CF3}$ with 1,3-bis(3-aminopropyl)-1,1,3,3-tetramethyldisiloxane in the presence of TMAH. The cured PSBPI produced optically transparent films with excellent thermal-oxidative stability, which were resistant to solvent and flexible. The characteristics of the PSBPI, due to microphase separation, was dependent on the content of APMFS in the PI backbone. CTE (α) and upper T_g for PSBPI decreased with increased content of APMFS. Also, Ra for the PSBPI reached a plateau at APMFS content of 10 wt %, and then gradually decreased to form a smooth surface.

This work has been supported by the Hyperstructured Organic Materials Research Center, which is gratefully acknowledged.

REFERENCES

1. Progar, D. J.; St. Clair, T. L. J Adhes 1987, 21, 35.
2. Yeats, R.; Von Dessoneck, K. Appl Phys Lett 1984, 44, 145.
3. Bessonov, M. J.; Koton, M. M.; Kudryavtsev, V. V.; Laius, J. A. Polyimides; Thermal Stable Polymers; Plenum: New York, 1987, 2nd ed.
4. Ghosh, K. L.; Mittal, K. L., Eds. Polyimides—Fundamentals and Applications; Dekker: New York, 1996.
5. Kuckertz, V. H. Macromol Chem Phys 1996, 4–5, 212.
6. William, M. C.; Spontak, R. J Appl Polym Sci 1989, 38, 1607.
7. Berger, A. U.S. Pat. 4,395,527 (1983).
8. Lee, C. J. U.S. Pat. 4,670,497 (1987).
9. Kang, D. W.; Kim, Y. M. J Ind Eng Chem 1999, 5, 4.
10. Ichika, H.; Machino, F.; Teranishi, H.; Ichikawa, T. Silicone-Based Polymer Science; Zeigler, J. M.; Fearon, F. W. G., Eds.; American Chemical Society: Washington, DC, 1990, p. 619.